

# Permutation Numbers

Vincenzo De Florio

Department of Electrical Engineering, University of Leuven,  
Kasteelpark Arenberg 10, 3001 Leuven-Heverlee, Belgium

---

This paper investigates some series of integers which are derived from a recursively defined sequence of permutations of words. Such a recursion can be interpreted as a dynamic system. Geometrical representations of these series appear to be self-similar, symmetrical, and factorizable. The paper also shows how some bidimensional images may be decomposed into images corresponding to permutations of fewer symbols.

---

## 1. Introduction

---

Any positive integer can be represented by a digit sequence in base  $b$ , and so it gives a permutation of the corresponding multiset. Depending on how many zeroes to the left of the first significant digit are used, you get a different multiset. Starting with a fixed multiset containing digits, one gets a list of numbers corresponding to its permutations. We investigate the dynamics of the permutation numbers corresponding to a successor operation on the permutations. We also introduce geometrical representations for some series of permutation numbers and show some of their properties.

The paper is structured as follows. In section 2 a formal model is introduced. Section 3 discusses some simple series of permutation numbers and their geometrical representations. Section 4 discusses other series that produce multidimensional geometrical representations and draws some observations on their structure. Conclusions are reported in section 5.

## 2. Formal model

---

In this section we introduce a formal model and a function. We show that the function is a successor for the lexicographically ordered generation of the permutations of a multiset.

**Definition 1.** Let us consider a set of symbols,  $\{a_1, \dots, a_m\}$ , with  $a_1 < \dots < a_m$ . Let  $M = \{\underbrace{a_1, \dots, a_1}_{c_1}, \dots, \underbrace{a_m, \dots, a_m}_{c_m}\} = \{a_1^{c_1}, \dots, a_m^{c_m}\}$  be a

multiset of  $n = \sum_{i=1}^m c_i$  elements, with  $\forall i \in \{1, \dots, m\} : c_i > 0$ . Any arrangements of the elements of  $M$  into a row is a *permutation of  $M$*  and is denoted as  $p^M$  (or, where  $M$  is implicit, as  $p$ ).

Element  $k$  in permutation  $p$  is denoted as  $p[k]$ . Arrangements are obtained through the “ $\cdot$ ” operator, concatenating symbols into “words” (strings of symbols). Let  $a^c$  be an abbreviated form for  $\overbrace{a \cdot a \cdots a}^c$ .

**Definition 2.** Given any two permutations  $p_1$  and  $p_2$  of the same multiset  $M$ , we say that  $p_1$  precedes  $p_2$  (denoted as  $p_1 < p_2$ ) if and only if  $\exists k \in \{1, \dots, n\} : (\forall j < k : p_1[j] = p_2[j]) \wedge (p_1[k] < p_2[k])$ .

**Definition 3.** The set of all different permutations of  $M$  is denoted as  $\mathcal{P}_M$  (or simply  $\mathcal{P}$  when  $M$  can be omitted with no risk of ambiguity).

Clearly  $\mathcal{P}_M$  is linearly ordered by the “ $<$ ” relation. Note also that  $|\mathcal{P}_M| = \binom{n}{c_1, \dots, c_m}$ , that is, the multinomial coefficient of  $n$  over the  $c_i$ .

**Definition 4.** The following permutation of  $M$ :

$$\underbrace{a_1 \dots a_1}_{c_1} \underbrace{a_2 \dots a_2}_{c_2} \cdots \underbrace{a_m \dots a_m}_{c_m} = a_1^{c_1} \cdot a_2^{c_2} \cdots a_m^{c_m}$$

is called the *zero permutation* of  $M$ , or briefly its *zero*, and is denoted as  $p_0^M$ , or simply  $p_0$ .

**Definition 5.** The following permutation of  $M$ :

$$\underbrace{a_m \dots a_m}_{c_m} \underbrace{a_{m-1} \dots a_{m-1}}_{c_{m-1}} \cdots \underbrace{a_1 \dots a_1}_{c_1} = a_m^{c_m} \cdot a_{m-1}^{c_{m-1}} \cdots a_1^{c_1}$$

is the *end permutation* of  $M$  and is denoted as  $p_\Omega^M$ , or simply  $p_\Omega$ .

Lemma 1 defines a Turing machine that finds out which subset of any input permutation should be shuffled in order to produce the “next” permutation in  $(\mathcal{P}_M, <)$ .

**Lemma 1.** Let  $p^M \in \mathcal{P}_M$  and  $a \in M$ . If  $p^M \neq p_\Omega^M$  then there exist two disjoint subsets of  $M$ , say  $L$  and  $R$ , such that:

1.  $p^M = p^L a p^R$ ,
2.  $a < \max\{b \mid b \in R\}$ ,
3.  $R \neq \emptyset$ .

*Proof.* Let us represent  $p^M$ , left-to-right, on the tape of a Turing machine [1], with the head on the rightmost symbol of  $p^M$ . Then let us instruct the machine to scan the permutation right-to-left, halting at the first couple of contiguous symbols which is not an inversion, or at the left of its leftmost character. (An inversion is any couple of contiguous characters  $xy$  such that  $x < y$ .) At the end of processing time the head of the machine may be in one of the following two states.

- Moved one position leftward. In this case, take  $R$  as the singleton consisting of the rightmost character in  $p^M$  (say  $z$ ),  $a$ ; as the symbol to its left, and  $L = \complement_M\{a, z\}$  (i.e., the complementary set of  $\{a, z\}$  with respect to  $M$ ).
- Moved somewhere else within the permutation, that is, the head's total number of shifts were more than one and less than  $n$ . In this case, let  $a$  be the symbol upon which the head stands; then let  $L$  and  $R$  be made of the elements represented by the two substrings respectively on the left and right of  $a$ . (Note that  $L$  may also be empty.)

The head should not be found on the left of the leftmost character of the permutation, because this would mean that no inversion had been found. In this case  $p^M$  would equal  $p_\Omega^M$ , contradicting the hypothesis. ■

**Definition 6.** From Lemma 1, if  $p \in \mathcal{P}_M, p \neq p_\Omega^M$ , then  $p$  can be decomposed into the form  $p^L a p_\Omega^R$  such that  $\exists b \in R : a < b$ . Now let  $c = \min\{b \in R \mid a < b\}$  and consider the set  $\overline{R} = \{a\} \cup \complement_R\{c\}$ . Then let the following permutation of  $p$ :

$$p' = p^L c p_\Omega^{\overline{R}}$$

be called the *successor* (or, the *next*) permutation for  $p$ . If  $p = p_\Omega$ , let  $p' = p_\Omega$ .

Note that if  $p \neq p_\Omega$ , then  $p^L$  is the invariant part of  $p$  with respect to the successor operator.

**Definition 7.** The following function:

$$\text{succ} : \mathcal{P} \rightarrow \mathcal{P},$$

such that  $\forall p \in \mathcal{P} : \text{succ}(p) = p'$ , is called the *successor function*.

**Definition 8.** Let us define the *powers of succ* as follows:

$$\forall p \in \mathcal{P} : \begin{cases} \text{succ}^0(p) = p \\ \text{succ}^x(p) = \text{succ}(\text{succ}^{x-1}(p)) \text{ if } x > 0. \end{cases}$$

Note that, given any permutation, zero or not, it is possible to recursively apply the successor operator on it, up to the end permutation. All strings obtained are different arrangements of the characters of the original string, that is, they are a subset (possibly an improper one) of its permutations. Such permutations can now be regarded as consecutive *orbits* of the successor operator on the original string.

Theorem 1 shows that the function **succ** is indeed a successor and, as such, it generates each and every permutation of  $M$ .<sup>1</sup>

---

<sup>1</sup>It is worth remarking the similarities between our definitions and those of Peano's axioms for arithmetics [2], based on the concepts of *zero*, *number*, and *successor*. A nice alternative way to refer to the permutation numbers could indeed be "Peano numbers"—after the words *permutation*, *anagram*, and *orbits*.

**Theorem 1.** For any multiset  $M$ , the number of different permutations that can be observed, starting from  $p_0$  and recursively applying the successor operator up to the end permutation, is equal to

$$|\mathcal{P}_M| = \left( c_1, c_2, \dots, c_n \right). \quad (1)$$

The proof, by induction on  $n$ , is omitted for the sake of brevity. One may refer, for example, to [3–7] for classical formulations of the same function.<sup>2</sup>

**Definition 9.** Let us consider a multiset  $M$  and its zero permutation  $p_0$ . Let us call the function  $\text{ord} : \mathcal{P} \rightarrow \mathbb{N}$  the *order of a permutation* such that

$$\begin{cases} \text{ord}(p_0) = 0 \\ \text{ord}(p) = z & \text{iff } p \neq p_0 \text{ and } p = \text{succ}^z(p_0). \end{cases}$$

**Definition 10.** Let  $p$  be a permutation of  $M$ . Let us call the *digit function* of  $p$  the function  $d_p : \{1, 2, \dots, n\} \rightarrow \{0, 1, \dots, m-1\}$ , defined as follows:

$$d_p(i) = j \quad \text{iff } p[i] = a_j.$$

**Definition 11.** Let  $\mathbb{N}$  represent the set of integer numbers. The function  $v : \mathcal{P}_M \rightarrow \mathbb{N}$ , such that

$$\forall p : v(p) = \sum_{k=1}^n d_p(k) \times m^{n-k},$$

is called the *numbering function* for  $M$ .  $v(p)$  is called the *number of permutation*  $p$ .

### 3. Permutation numbers and their representations

Various series can be derived starting from the successor function  $\text{succ}$  and its orbits. Three of those series and their representations are the subject of this section.

#### 3.1 Permutation numbers

Let us consider the following series:

$$e_M = \left( v(p_M) \right)_{p_M = \text{succ}^i(p_0), i > 0}.$$

Series  $e_M$ , or  $e$  for short, is the series of the permutation numbers, that is, the monotonically increasing series of integer numbers that one can compose using a fixed digit distribution.

<sup>2</sup>As the reader may have noticed already, the focus here is not on the generating algorithm but on its reformulation as a complex system.

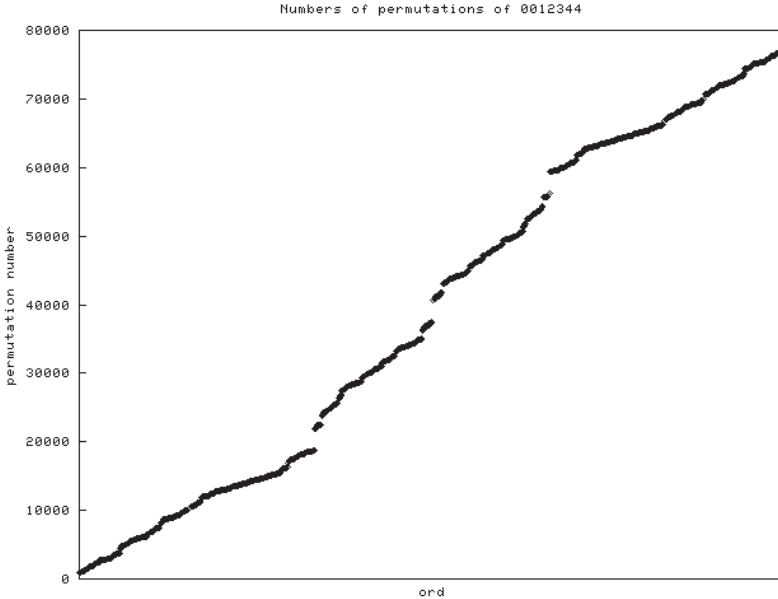


**Figure 1.**  $E(0012344)$ . Note the symmetry.

A straightforward representation for  $e$  is given by plotting couples  $(ord(p_M), v(p_M))$  for each valid  $p_M \in \mathcal{P}_M$ . Let us call  $E(p_0^M)$  the *graph* of  $e$  for multiset  $M$ .

Figures 1 through 4 represent  $e$  for various values of  $M$ . In general one may observe that graphs of multisets whose symbol distribution depicts some regularity are symmetrical, while “irregular” graphs, in some cases, may reveal self-similarities.

■ **3.2 Series  $d$  and  $r$**

**Definition 12.** Let us define the function  $\delta_M : M \rightarrow \mathbf{N}$  such that

$$\forall p \neq p_\Omega : \delta_M(p) = v(p') - v(p).$$

The function  $\delta$ , measuring the distance between the number of permutation  $p'$  from that of permutation  $p$ , is called the *distance function*.

Let us call  $d$  the following series:

$$d = D e = (\delta_M(p_M))_{p_M = \text{succ}^i(p_0), i > 0}$$

Note how  $\delta$  specifies the number to be added to the number of the current permutation in order to produce the number of the next permutation.

Figure 5 shows two graphs for the couples  $(ord(p_M), \delta_M(p_M))$  for each  $p \in \mathcal{P}_M$ , when  $M$  is  $\{0, 1, 2, 3, 4\}$  and  $\{0, 1, 2, 3, 4, 5\}$ . Let us call such

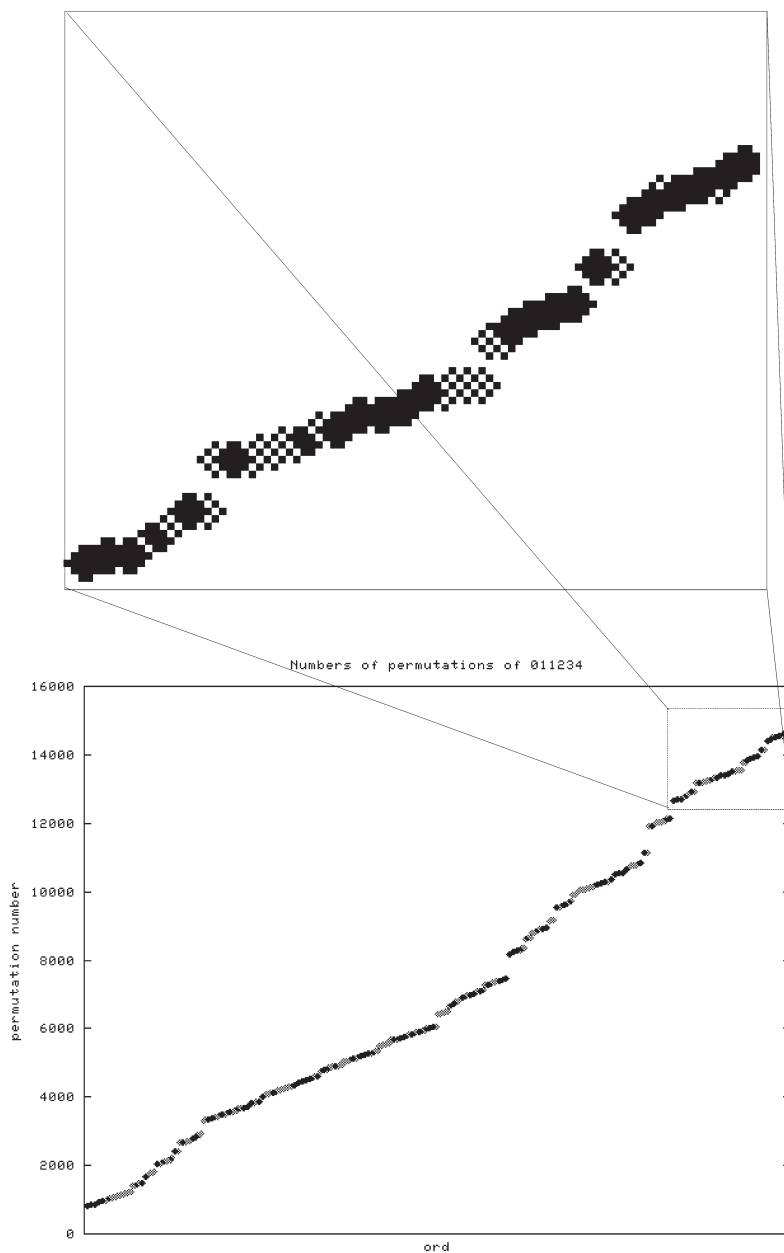


**Figure 2.**  $E(011234)$ . The top-right part has been magnified in order to show the self-similarity of the graph.

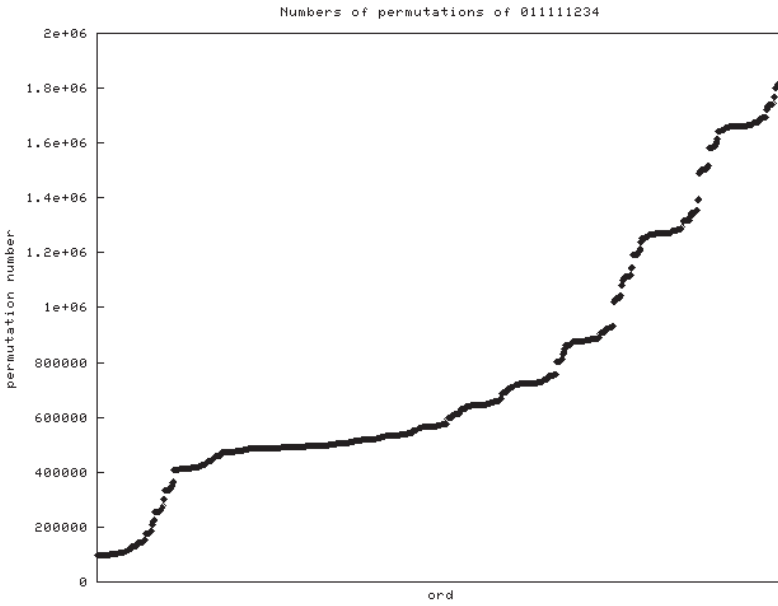


Figure 3.  $E(011111234)$ .

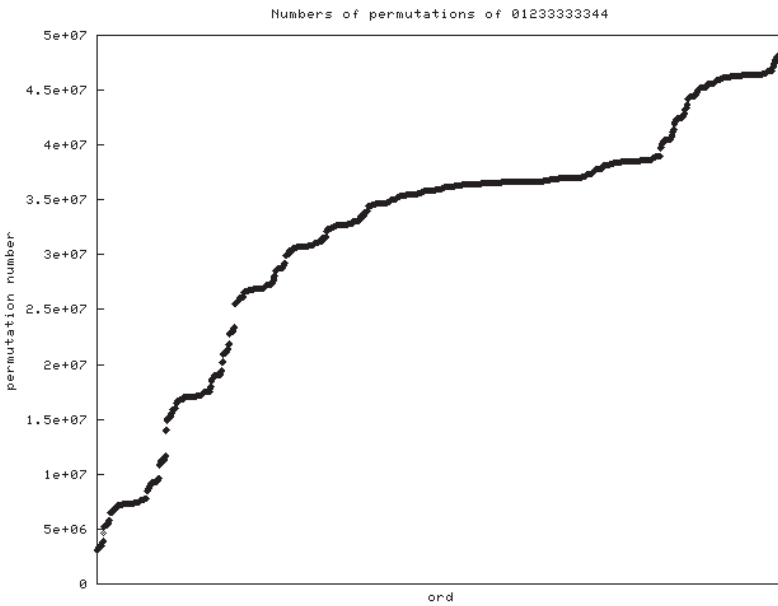
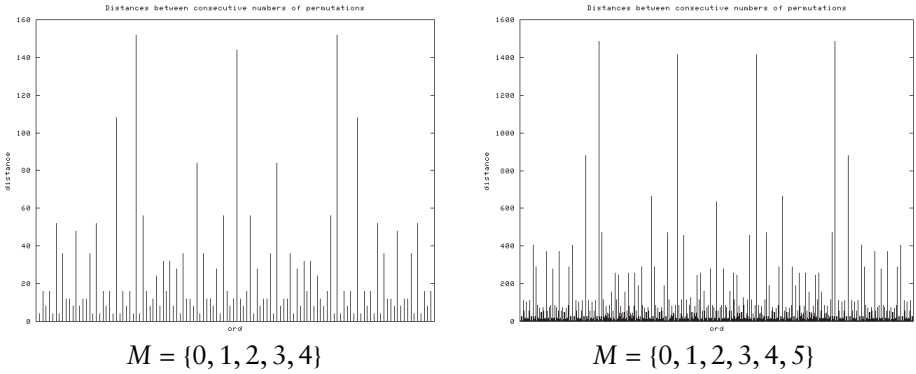
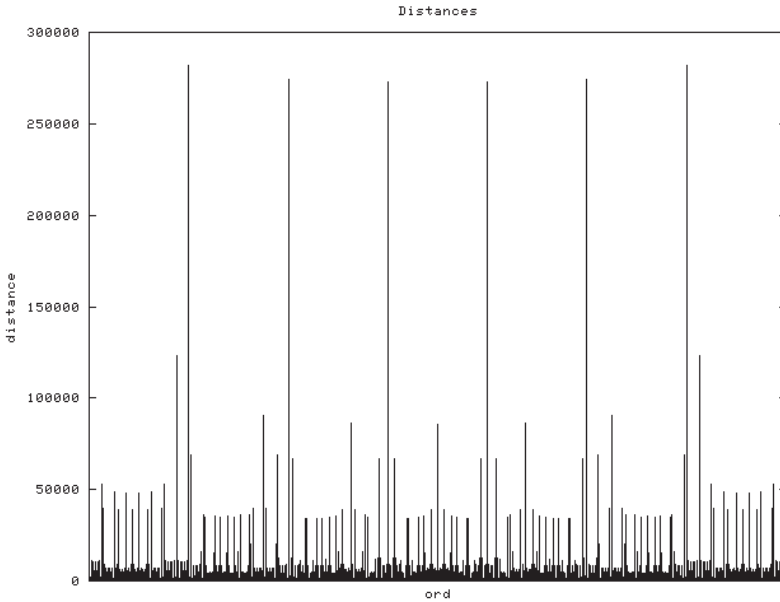


Figure 4.  $E(01233333344)$ .



**Figure 5.** Graphs of  $\delta(p) = v(p') - v(p)$  for  $p = p_0$  to  $p_\Omega$  when  $M$  is  $\{0, 1, 2, 3, 4\}$  and  $\{0, 1, 2, 3, 4, 5\}$ . Note the symmetry and self-similarity.



**Figure 6.**  $D(01234567)$ .

graphs  $D(p_0^M)$ . Figures 6 through 11 show other examples. It is also possible to observe symmetry and self-similarity in this case.

**Definition 13.** Let us define the function  $\varrho_M : M \rightarrow \mathbf{N}$ , such that

$$\forall p \neq p_\Omega, \quad p = p^L a p_\Omega^R : \varrho_M(p) = |R|.$$

As described in Lemma 1 and Definition 6, any  $p \in \mathcal{P}$  may be decomposed into a left-hand part, remain untouched by the **succ** operator,



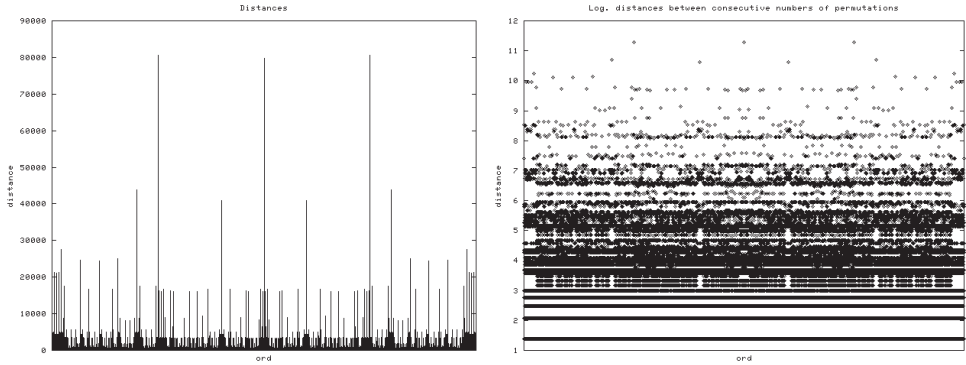


**Figure 7.**  $D(0011223344)$  and  $\log D(0011223344)$ .

and a right-hand part (called  $R$  in Lemma 1), which on the contrary is affected by  $\text{succ}$ . The function  $\varrho$  returns the cardinality of  $R$ .

**Definition 14.** Let us call  $r$  the following series:

$$r = (\varrho_M(p_M))_{p_M = \text{succ}^i(p_0), i > 0}$$

A representation for  $r$  is given by plotting couples  $(\text{ord}(p_M), \varrho_M(p_M))$  for each valid  $p_M \in \mathcal{P}_M$ . Table 1 shows histograms of  $r$  in four simple cases.

Let us call  $R(p_0^M)$  the graph of  $r$  for multiset  $M$ . Observing those graphs, one may note how  $r$  verifies the following properties.

1. When  $M$  consists of only two classes of symbols,  $c_1$  and  $c_2$ , the corresponding graphs for  $R(a_1^j \cdot a_2^k)$  and  $R(a_1^k \cdot a_2^j)$  are “specular twins”—just like Tweedledee and Tweedledum in Carroll’s *Through the Looking Glass*.
2. When the distribution of classes is symmetrical, so it is for the corresponding graphs.
3. Graphs are factorizable according to the following decomposition rule:

$$R(a_1^{c_1} \cdot a_2^{c_2} \dots a_m^{c_m}) \rightarrow R(a_1^{c_1-1} \cdot a_2^{c_2} \dots a_m^{c_m}), R(a_1^{c_1} \cdot a_2^{c_2-1} \dots a_m^{c_m}), \dots, R(a_1^{c_1} \cdot a_2^{c_2} \dots a_m^{c_m-1}).$$

Note that when  $M$  consists of two classes of symbols the decomposition rule produces a binary tree whose coefficients constitute a Pascal triangle. Hence, it is possible to make use of powers of polynomials to represent decomposition schemes. For instance, here is the decomposition rule for permutations with just two classes, let us call them  $a$  and  $b$ . Let  $x = \min\{i, j\}$ . Then

$$R(a^i \cdot b^j) \equiv R(a^i \cdot b^j \times (a + b)^0) \rightarrow R(a^{i-1} \cdot b^{j-1} \times (a + b)) \rightarrow \dots \rightarrow R(a^{i-x} \cdot b^{j-x} \times (a + b)^x),$$

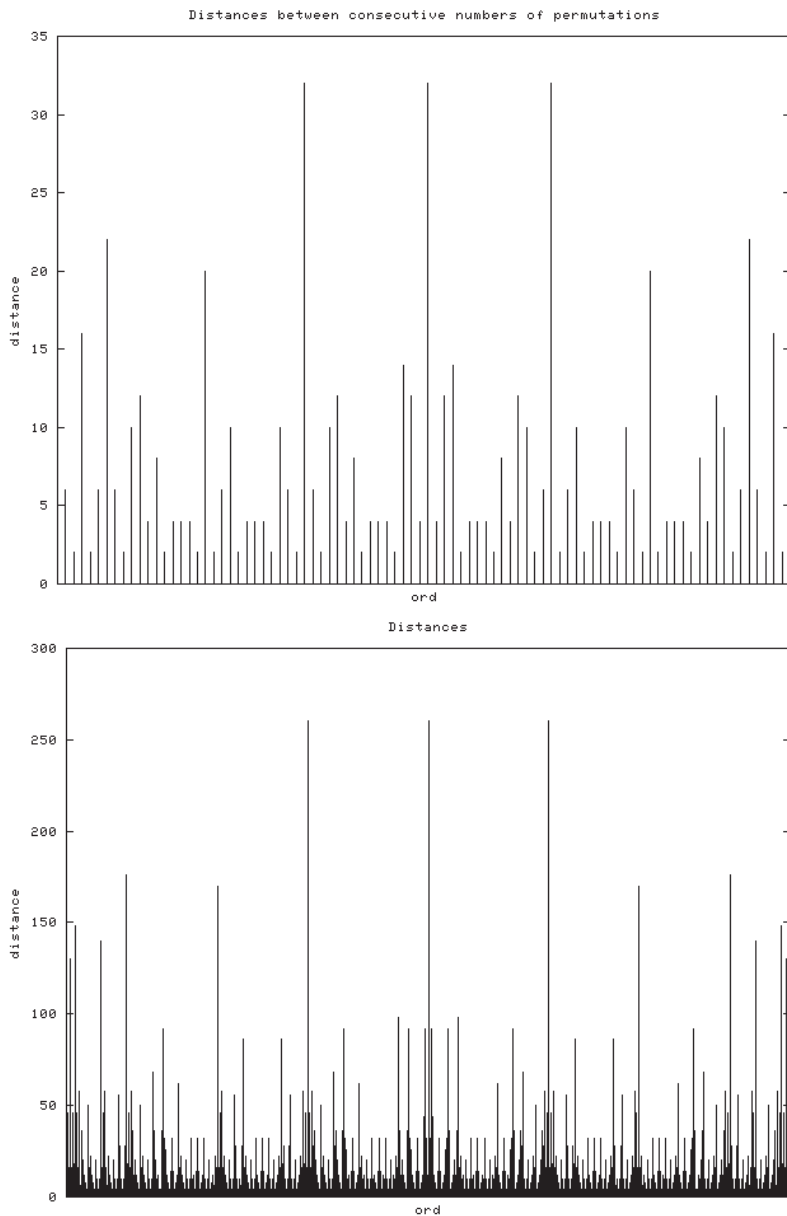


**Figure 8.** Graphs of  $\delta$  when  $M = \{2 \times 0, 2 \times 1, 2 \times 2\}$  and  $\{3 \times 0, 3 \times 1, 3 \times 2\}$ . This case also shows symmetry and self-similarity.

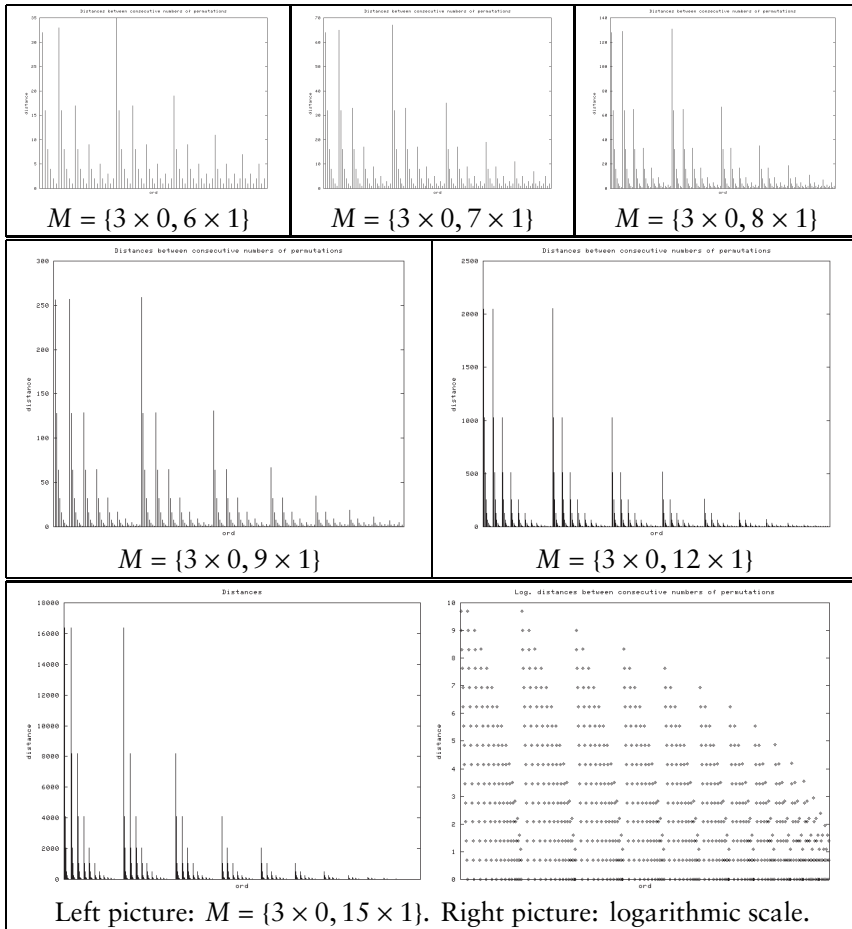


**Figure 9.** A fixed number of zero digits and an increasing number of one digits. No symmetry is evident in this case. All pictures portray a self-similar decaying oscillation pattern.

where the products are between schemes of permutation and powers of binomials and produce the schemes of the permutations of the decompositions.

Figure 12 shows the factorizations applied to the permutations of  $M = \{0^3 1^3\}$ .

When there are three classes of symbols, say  $a$ ,  $b$ , and  $c$ , the corresponding rule is:  $\forall x \leq \min\{i, j, k\}$ ,

$$\begin{aligned}
 a^i b^j c^k &\equiv a^i b^j c^k \times (bc + ac + ab)^0 \rightarrow a^{i-1} b^{j-1} c^{k-1} \times (bc + ac + ab) \\
 &\rightarrow \dots \rightarrow a^{i-x} b^{j-x} c^{k-x} \times (bc + ac + ab)^x.
 \end{aligned}$$

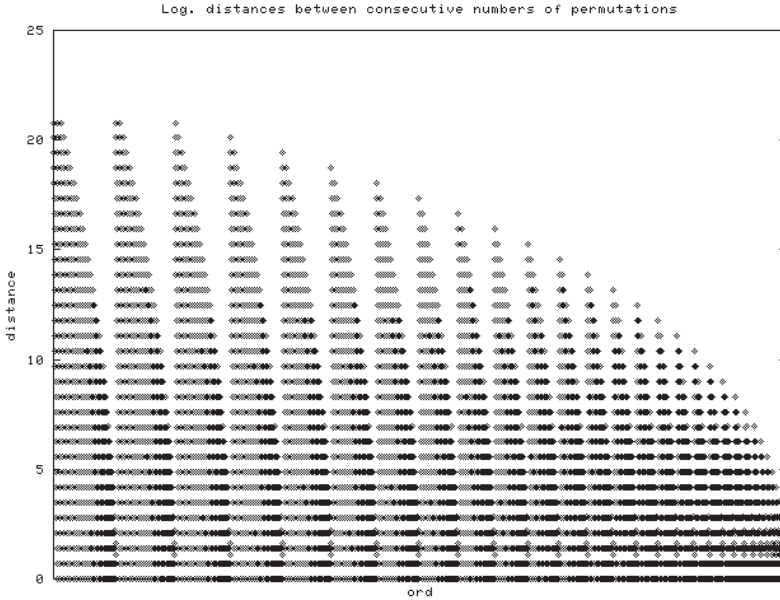


Figure 10.  $\log D(0^3 1^{32})$ .

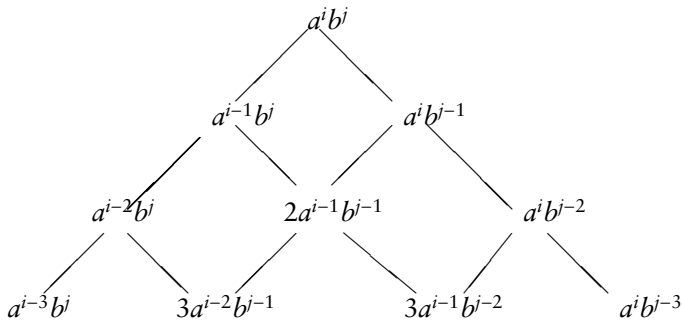


Figure 11. Decomposition of  $a^i b^j$ ,  $i > 4, j > 4$ .

In general, the decomposition rule for permutations of symbols belonging to  $m$  classes appears to be,  $\forall x \leq \min\{c_1, c_2, \dots, c_m\}$ :

$$p = \prod_{i=1}^m a_i^{c_i} = a_1^{c_1} a_2^{c_2} \dots a_m^{c_m} = a_1^{c_1-x} a_2^{c_2-x} \dots a_m^{c_m-x} \times \left( \sum_{r=1}^m \prod_{s \neq r} a_s \right)^x.$$

perm 001111 ..... 010111 ..... 011011 ..... 011101 ..... 011110 ..... 100111 ..... 101011 ..... 101101 ..... 101110 ..... 110011 ..... 110101 ..... 110110 ..... 111001 ..... 111010 ..... 111100 .....	perm 000011 ..... 000101 ..... 000110 ..... 001001 ..... 001010 ..... 001100 ..... 010001 ..... 010010 ..... 010100 ..... 011000 ..... 100001 ..... 100010 ..... 100100 ..... 101000 ..... 110000 .....
perm 000111 ..... 001011 ..... 001101 ..... 001110 ..... 010011 ..... 010101 ..... 010110 ..... 011001 ..... 011010 ..... 011100 ..... 100011 ..... 100101 ..... 100110 ..... 101001 ..... 101010 ..... 101100 ..... 110001 ..... 110010 ..... 110100 ..... 111000 .....	perm 01112 ..... 01121 ..... 01211 ..... 02111 ..... 10112 ..... 10121 ..... 10211 ..... 11012 ..... 11021 ..... 11102 ..... 11120 ..... 11201 ..... 11210 ..... 12011 ..... 12101 ..... 12110 ..... 20111 ..... 21011 ..... 21101 ..... 21110 .....

**Table 1.** Here  $r$  is portrayed as histograms in order to facilitate some observations: Note how  $R(a^i \cdot b^k)$  and  $R(a^k \cdot b^i)$  are specular; how  $R(a^i \cdot j)$  is symmetrical; how it is possible to “factorize”  $R(a^i \cdot b^k)$  into  $R(a^{i-1} \cdot b^k)$ ,  $R(a^i \cdot b^{k-1})$  and  $R(a^i \cdot b^i \cdot c^k)$  into  $R(a^{i-1} \cdot b^i \cdot c^k)$ ,  $R(a^i \cdot b^{i-1} \cdot c^k)$ ,  $R(a^i \cdot b^i \cdot c^{k-1})$ .

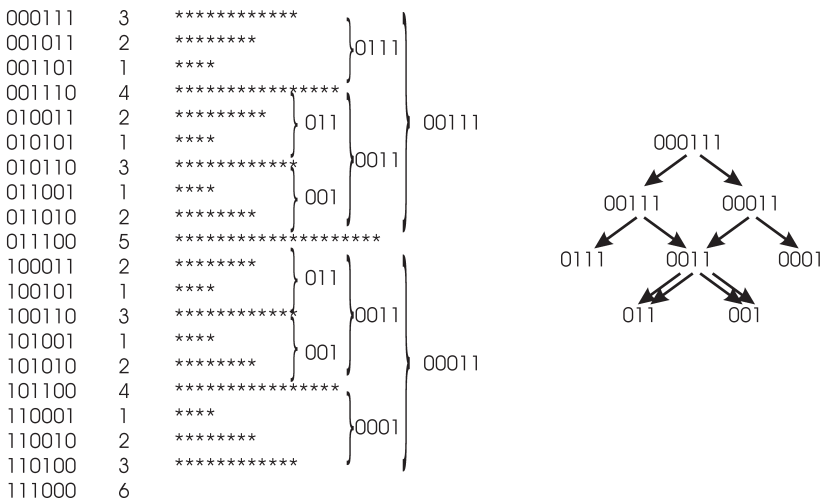


**Figure 12.** Factorizations of  $M = \{0^3 1^3\}$ .

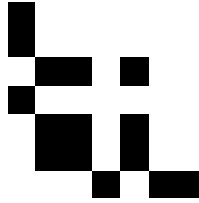


**Figure 13.** HeartQuake numbers for  $M = \{0^4, 1^2\}$  and two equal-sized blocks ( $b = 2$ ).

**4. HeartQuake numbers**

In the rest of the paper the focus is on another series of numbers obtained by splitting the multiset into blocks and computing the permutation number of those blocks.

**Definition 15.** For each multiset  $M$  let us consider a partition of  $M$  into  $b$  blocks,  $b > 1$ ,  $M_1, \dots, M_b$ . Then consider the following tuple:

$$h = \left( v_M(p_{M_1}), \dots, v_M(p_{M_b}) \right)_{\forall p_{M_1}, \dots, \forall p_{M_b}}.$$

Tuple  $h$  is called the *tuple of the HeartQuake numbers*.

The name “HeartQuake numbers” comes after that of a family of games of cards with two players, its combinatorial space being that of Definition 15 when  $b = 2$  [8].

A representation of the HeartQuake numbers, given a particular collection of blocks  $M_j$ , is obtained by plotting tuples  $(v(p_{M_1}), \dots, v(p_{M_b}))$  in  $b$ -dimensional euclidean space.

In the following we concentrate our attention on the cases  $b = 2$  and  $b = 3$ .

**4.1 Bidimensional HeartQuake numbers**

This section focuses on HeartQuake numbers with  $b = 2$ , that is,

$$h = \left( v(p_{M_1}), v(p_{M_2}) \right)_{\forall p_{M_1}, \forall p_{M_2}}.$$

An example of the graphs of  $h$  can be seen in Figure 13.

**4.1.1 Up to two classes of symbols**

Let us first consider the subcase where  $M$  contains an even number of elements, each either 0 or 1. Then the possibilities for  $M$  can be represented as nonnegative pairs  $(c_1, c_2)$  where  $c_1$  is the number of zeroes,  $c_2$  is the number of ones, and  $c_1 + c_2$  is even.

In so doing, the spectrum of all possible permutations can be represented as the following matrix:

$$\begin{pmatrix} & (0, 2) & (0, 4) & \dots & \\ (1, 1) & (1, 3) & (1, 5) & \dots & \\ (2, 0) & (2, 2) & (2, 4) & \dots & \\ (3, 1) & (3, 3) & (3, 5) & \dots & \\ (4, 0) & (4, 2) & (4, 4) & \dots & \\ & \vdots & \vdots & \vdots & \end{pmatrix}, \tag{2}$$

where in each couple  $(x, y)$ ,  $x$  represents the values of  $c_1$  and  $y$  that of  $c_2$ . A value of zero means that the corresponding symbol is not part of the multiset.

Let us call  $\mathcal{H}_{x,y}$  the graph of  $(x, y)$ .

Figure 14 depicts 15 images of equation (2) and can be used to make a number of observations. Let  $r$  and  $c$  be any two integers such that  $r + c$  is even.

**Observation 1.** For any  $r > 0$  and  $c > 0$ :  $\mathcal{H}_{r,c}$  can be partitioned into four equal-sized regions.

This is clearly visible, for example, in the two last rows of Figure 14.

**Observation 2.** For any  $r$  and  $c$ : the pattern represented in  $\mathcal{H}_{r,c}$  is one of those contained in  $\mathcal{H}_{r,c+2}$ , that is, every graph is fully contained in its right neighbor.

This is shown, for example, in Figures 14 and 15.

**Observation 3.** The four patterns in  $\mathcal{H}_{r,c}$  are the same as those in the following images:  $\mathcal{H}_{r-2,c}$ ,  $\mathcal{H}_{r-1,c-1}$ , and  $\mathcal{H}_{r,c-2}$ . Patterns are arranged according to the following scheme:

$$\begin{pmatrix} \mathcal{H}_{r-1,c-1} & \mathcal{H}_{r,c-2} \\ \mathcal{H}_{r-2,c} & \mathcal{H}_{r-1,c-1} \end{pmatrix},$$

that is, a  $2 \times 2$  matrix in which the diagonal contains the one repeated pattern.

Another way to represent this is as:

$$\mathcal{H}_{r,c} = \mathcal{H}_{r-2,c} + 2\mathcal{H}_{r-1,c-1} + \mathcal{H}_{r,c-2}. \tag{3}$$

Note that equation (3) represents a relationship between images of  $r+c$  symbols and images with two symbols less. Iterating the process, one may factorize any  $\mathcal{H}_{r,c}$  into a number of atomic patterns, or patterns that cannot be further decomposed. Such patterns are all arranged in a frame made of the first two rows and the first two columns of equation (2).

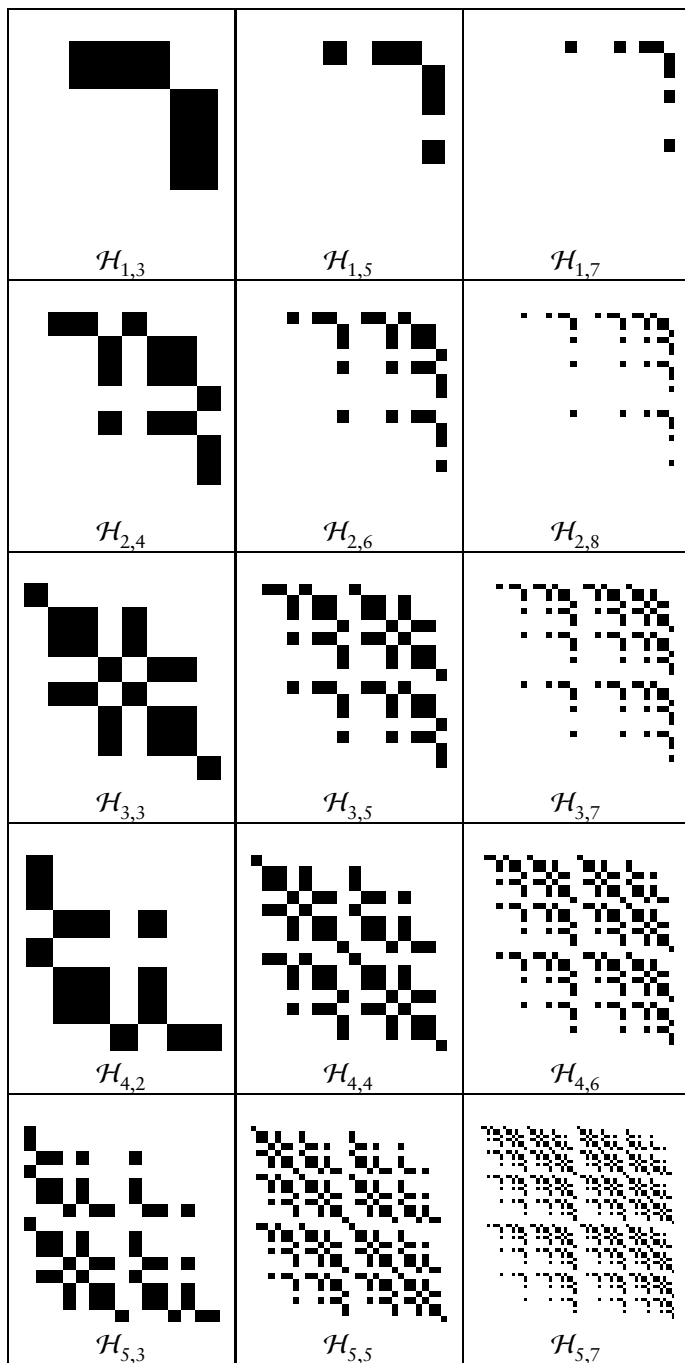


Figure 14. HeartQuake images.



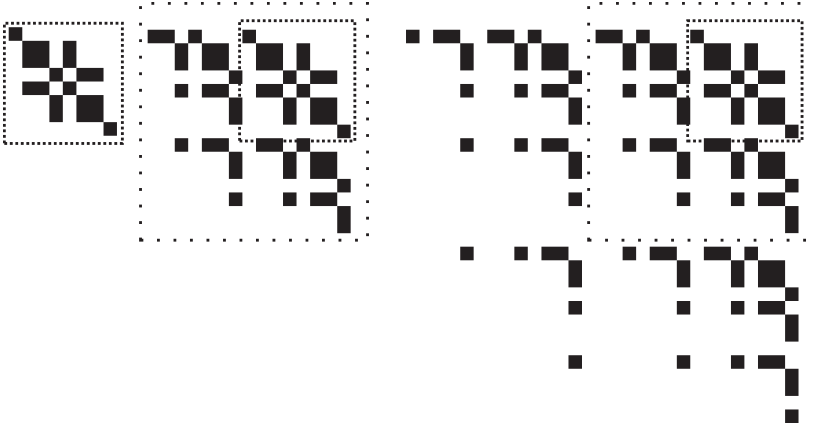


Figure 15.  $\mathcal{H}_{3,3}$ ,  $\mathcal{H}_{3,5}$ , and  $\mathcal{H}_{3,7}$ .

Moreover, given any  $r > 2$  and  $c > 2$ , the decomposition of  $\mathcal{H}_{r,c}$  is a linear combination of images  $\mathcal{H}_{0,i}$ ,  $\mathcal{H}_{1,i}$ ,  $\mathcal{H}_{j,0}$ , and  $\mathcal{H}_{j,1}$  with  $i \leq c$  and  $j \leq r$ . For example,  $\mathcal{H}_{8,6}$  can be factorized<sup>3</sup> into the following atomic patterns:

$$\begin{aligned} \mathcal{H}_{8,6} = & \mathcal{H}_{0,6} + 8 \times \mathcal{H}_{1,5} + 28 \times \mathcal{H}_{0,4} + 112 \times \mathcal{H}_{1,3} + 210 \times \mathcal{H}_{0,2} \\ & + 420 \times \mathcal{H}_{1,1} + 210 \times \mathcal{H}_{2,0} + 196 \times \mathcal{H}_{3,1} + 70 \times \mathcal{H}_{4,0} \\ & + 50 \times \mathcal{H}_{5,1} + 15 \times \mathcal{H}_{6,0} + 6 \times \mathcal{H}_{7,1} + \mathcal{H}_{8,0}. \end{aligned} \tag{4}$$

Figure 16 shows the distribution of the basic building blocks of  $\mathcal{H}_{8,6}$  within equation (2), while Figure 17 shows its decomposition tree.

**Observation 4.**  $\forall r, c : \mathcal{H}_{r,c}$  is specular to  $\mathcal{H}_{c,r}$ , that is,  $\mathcal{H}$  and its transpose depict equal patterns up to a resizing and a rototranslation.

This is clearly visible comparing couples of images in Figure 14. Figure 18 shows three such couples.

**Observation 5.** Some images depict a certain degree of self-similarity.

As an example, see Figure 19, which depicts  $\mathcal{H}_{8,6}$ .

**4.1.2 More than two classes of symbols**

This section focuses on the HeartQuake numbers of permutations with  $m > 2$ .

<sup>3</sup>The following short *Mathematica* program, courtesy of the reviewers of this paper, can be used to factorize the expressions of the HeartQuake graphs for  $k = 2, b = 2$ .

```
hfactorize[expr_] := FixedPoint[Expand[# /. h[x_, y_] /; Min[x,y] > 1
    -> h[x - 2, y] + 2h[x - 1, y - 1] + h[x, y - 2]] &, expr]
```

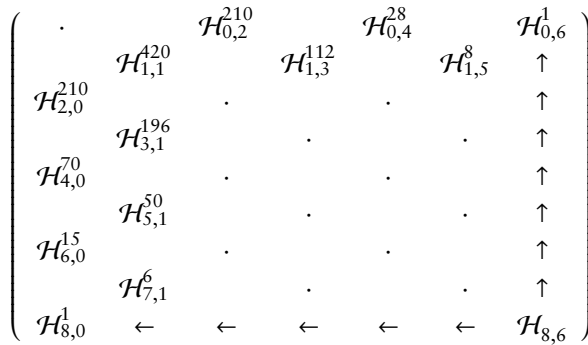


**Figure 16.** The basic blocks of image  $\mathcal{H}_{8,6}$ .  $\mathcal{H}_i^k$  means  $k$  occurrences of pattern  $\mathcal{H}_i$ . The symbol “ $\cdot$ ” here means “pattern not involved.”

A number of observations made for the cases of  $m = 1$  and  $m = 2$  can be extended to the general case. For example, for  $m = 3$ , images appear to consist of nine regions. Such regions represent patterns of other images according to the following rule of decomposition:

$$\begin{aligned}
 \mathcal{H}_{i,j,k} &= 2\mathcal{H}_{i-1,j,k-1} + 2\mathcal{H}_{i,j-1,k-1} + 2\mathcal{H}_{i-1,j-1,k} \\
 &+ \mathcal{H}_{i,j-2,k} + \mathcal{H}_{i-2,j,k} + \mathcal{H}_{i,j,k-2}.
 \end{aligned}
 \tag{5}$$

For an example, see Figure 20 showing image  $\mathcal{H}_{6,4,2}$  indicating its first-level regions. Moreover, note  $\mathcal{H}_{6,3,1}$  and the third region in the first row of  $\mathcal{H}_{5,3,2}$ , that is,  $\mathcal{H}_{5,2,1}$ .

In permutations with a class consisting of exactly two symbols, a collapse phenomenon occurs. One of the regions of the decomposition is the pattern of a permutation with one class less than in the original, that is, if the original image was from a permutation for which  $b = 3$ , that region belongs to a permutation for which  $b = 2$ . This phenomenon is observable in Figure 20: the region labeled  $\mathcal{H}_{6,4}$  is clearly one for which  $b = 2$ . Further decomposing such regions according to equation (3) it is possible to obtain images of permutations for which  $b = 1$ .

Another interesting phenomenon occurs in images like  $\mathcal{H}_{6,3,1}$  and  $\mathcal{H}_{5,2,1}$ , that is, images of permutations in which at least one class of symbols appears just once (see Figure 21). Applying equation (5) to image  $\mathcal{H}_{6,3,1}$  one gets

$$\mathcal{H}_{6,3,1} = \underbrace{2\mathcal{H}_{5,3} + 2\mathcal{H}_{6,2}}_{\text{collapse to } b=2 \text{ images}} + 2\mathcal{H}_{5,2,1} + \mathcal{H}_{6,1,1} + \mathcal{H}_{4,3,1} + \underbrace{\mathcal{H}_{6,3,-1}}_{\text{impossible!}}.$$

In other words, the decomposition rules still apply, and this leads to “imaginary” regions, such as  $\mathcal{H}_{6,3,-1}$ , which cannot be visualized and hence become empty regions.

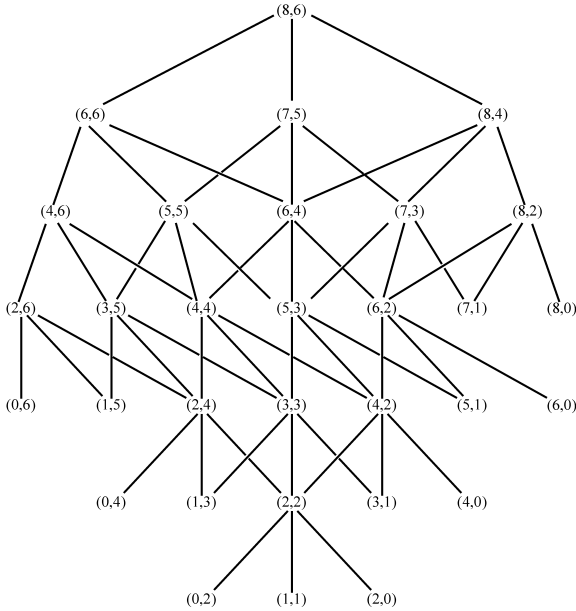


**Figure 17.** Decomposition tree for image  $\mathcal{H}_{8,6}$ . Note how the leaves are the “atomic patterns” in equation (4).

Is it possible to generalize the decomposition rule to images for which  $b > 2$ ? Experimental results suggest that, for any integer  $b > 2$ , a  $b$ -class,  $n$ -symbol HeartQuake image can be decomposed into a matrix of  $b \times b$  regions. This decomposition can be made as follows:  $b$  single regions of  $n - 2$  symbols each are disposed through the main diagonal and  $b \times (b - 1)/2$  double regions of  $n - 2$  symbols, each symmetrically located with respect to the main diagonal. More precisely: given  $I_k = \{0, 1, \dots, k - 1\}$  a set of indexes, let us denote with  $\{i\}$  the generic singleton and with  $\{i, j\}$  the generic subset of two elements of  $I_k$ . Experimental results show that the general decomposition rule is:

$$\mathcal{H}_{v_0, v_1, \dots, v_{b-1}} = \sum_{\{i\} \subset I_b} \mathcal{H}_{v_{a < i}, v_{i-2}, v_{i < b}} + 2 \sum_{\{i, j\} \subset I_b, i < j} \mathcal{H}_{v_{a < i}, v_{i-1}, v_{i < b < j}, v_{j-1}, v_{j < c < b}} \quad (6)$$

Equation (6) is consistent with previously described equations (3) and (5). Likewise, it again represents a relationship between images of permutations of  $r + c$  symbols and images of permutations with two symbols less. The process may be iterated producing patterns that are “atomic” for  $H_b$ , the extension of equation (2). Such patterns inherit the same distribution of those in equation (2): they lie in the first two superficial strata of the hypercube. Moreover, given any image in  $H_b$ , its basic patterns are localizable with the same method shown in Figure 16.

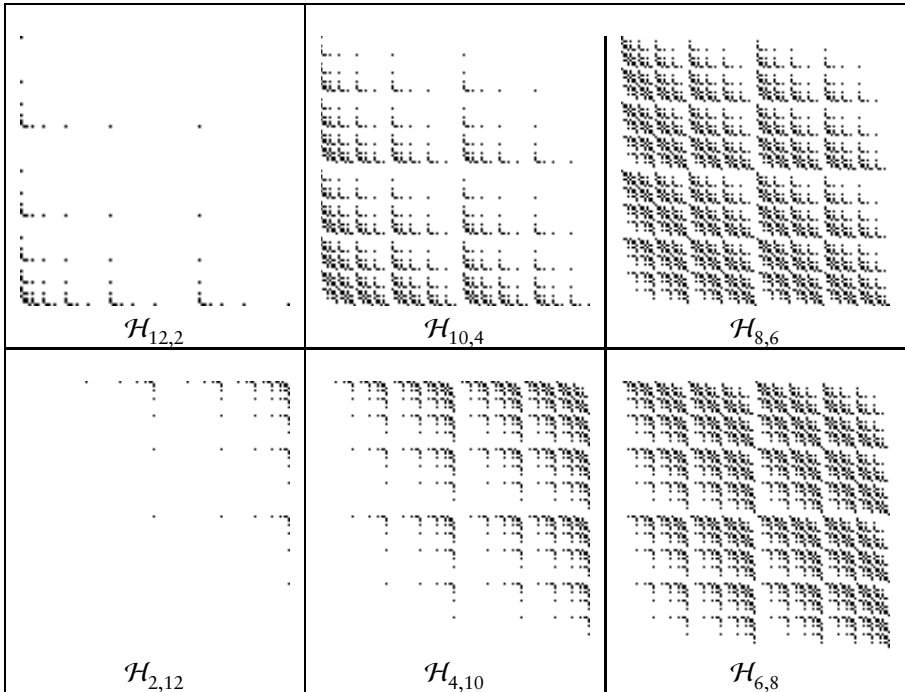


**Figure 18.** A set of images of HeartQuake numbers with  $n = 14$  and  $m = 2$ . Ignoring dimension and rotation, images  $\mathcal{H}_{(i,i)}$  and  $\mathcal{H}_{(j,i)}$  depict the same pattern.

#### 4.2 Three-dimensional graphs

HeartQuake numbers with  $b = 3$ , that is,

$$\mathbf{h} = \left( v_{M_1}(p_{M_1}), v_{M_2}(p_{M_2}), v_{M_3}(p_{M_3}) \right)_{\forall p_{M_1}, \forall p_{M_2}, \forall p_{M_3}},$$

are a case worth considering mainly because of their natural mapping to tridimensional images. Examples of the graphs of  $\mathbf{h}$  can be seen in Figures 22 and 23.<sup>4</sup>

### 5. Conclusions

This paper has introduced a number of series, all stemming from a simple recursive procedure that generates permutations of words. Such a recursive procedure can be interpreted as a dynamic system in which the permutations represent the orbits of a permutation-successor operator. Some geometrical representations for that dynamic system have

<sup>4</sup>Rendering was done with the Persistence of Vision ray-tracer, available at <http://www.povray.org>.

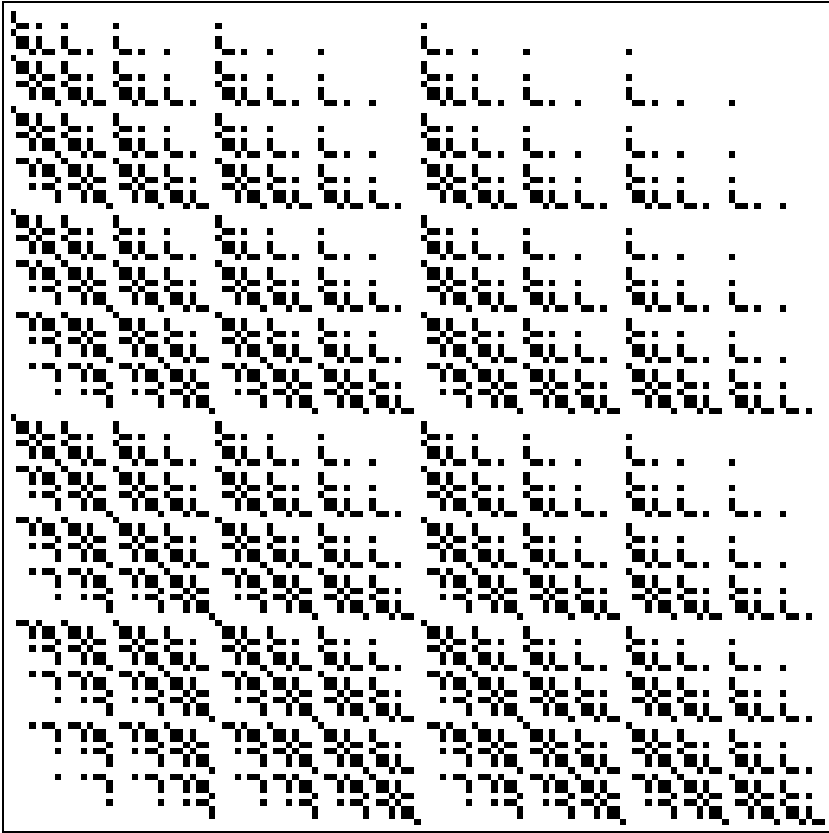


Figure 19. Image  $\mathcal{H}_{8,6}$ .

also been introduced, which exhibit complex properties such as self-similarity, symmetry, and factorizability. Yet another example of the emergence of complex structures from simple rules or algorithms [9, 10] has been provided and discussed.

### Acknowledgment

My gratitude goes to Tiziana for her Love and patience. Many thanks are due to the reviewers for their many helpful contributions to this paper.

### References

- [1] A. M. Turing, "On Computable Numbers, With an Application to the Entscheidungsproblem," *Proc. London Math. Soc.*, **42** (1936) 230–265.

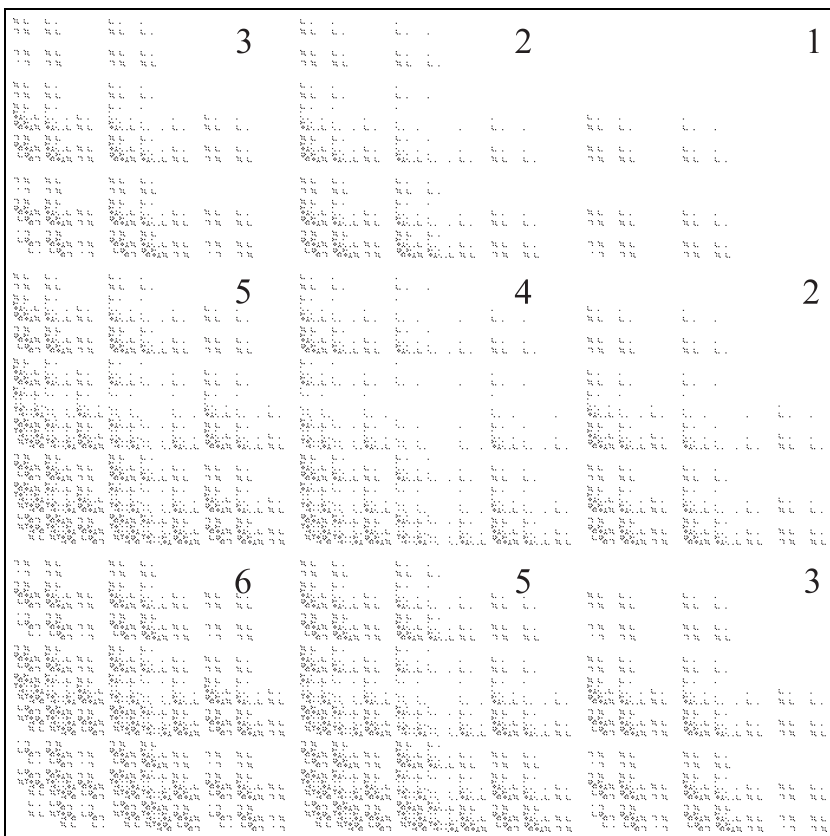


**Figure 20.** Image  $\mathcal{H}_{6,4,2}$ . Note the self-similarity. First-level regions of the decomposition are  $\mathcal{H}_{6,4}$  (1.),  $\mathcal{H}_{5,4,1}$  (2.),  $\mathcal{H}_{6,3,1}$  (3.),  $\mathcal{H}_{4,4,2}$  (4.),  $\mathcal{H}_{5,3,2}$  (5.), and  $\mathcal{H}_{6,2,2}$  (6.).

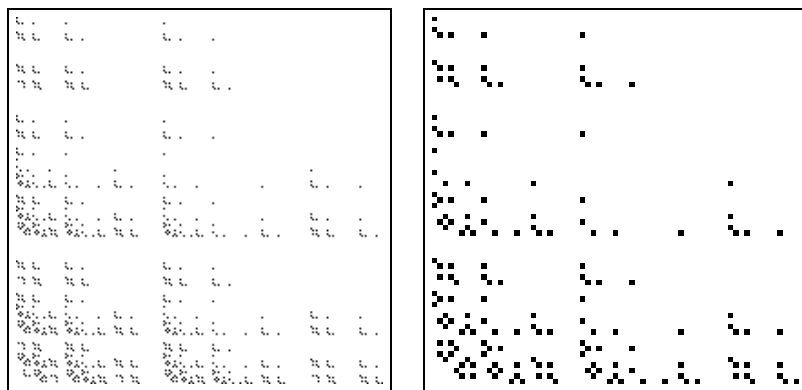


**Figure 21.** Images  $\mathcal{H}_{6,3,1}$  and  $\mathcal{H}_{5,2,1}$ . Note the similarity and the empty (“imaginary”) region on the right top of both images.

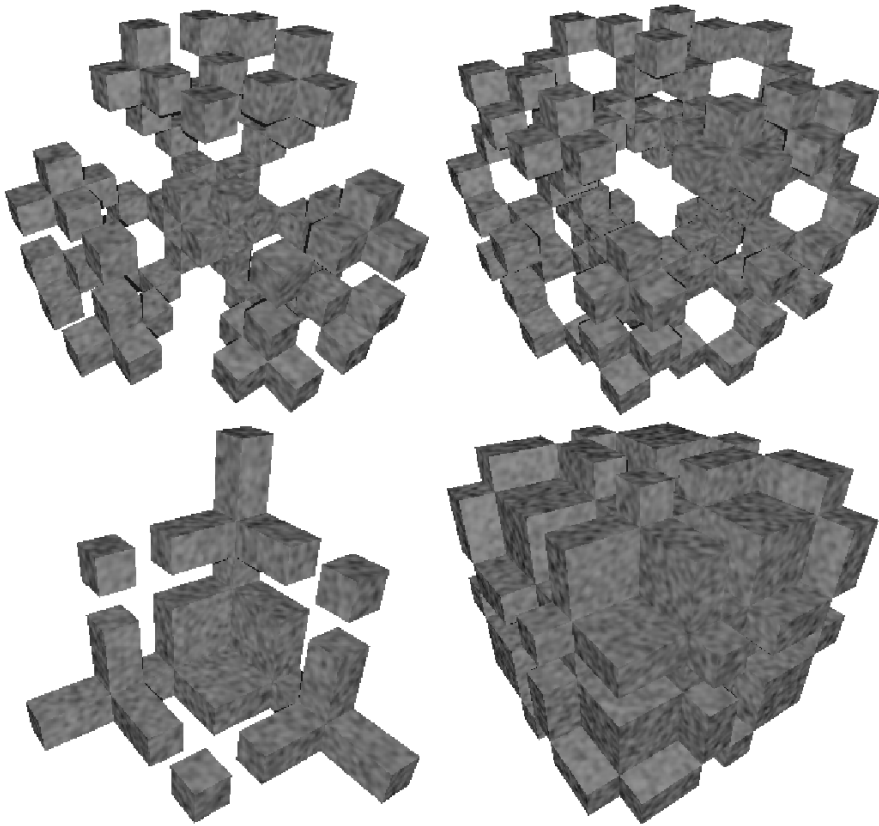


**Figure 22.** HeartQuake images of  $\mathcal{H}_{3,2,1}$  (top left),  $\mathcal{H}_{2,2,2}$  (top right),  $\mathcal{H}_{7,2}$  (bottom left), and  $\mathcal{H}_{4,5}$  (bottom right).

- [2] D. A. Gillies, *Frege, Dedekind, and Peano on the Foundations of Arithmetic* (Assen, 1982).
- [3] G. Herlich, “Four Combinatorial Algorithms,” *Communications of the ACM*, 16 (1973) 690–691.
- [4] G. Herlich, “Loopless Algorithms for Generating Permutations, Combinations, and Other Combinatorial Configurations,” *Journal of the ACM*, 20(3) (1973) 500–513.
- [5] D. E. Knuth, *The Art of Computer Programming, Volume 1: Fundamental Algorithms* (Addison-Wesley, Reading MA, second edition, 1973).
- [6] M. Lothaire, *Combinatorics on Words* (Addison-Wesley, Reading, MA, 1983).
- [7] E. S. Page and L. B. Wilson, *An Introduction to Computational Combinatorics* (Cambridge University Press, Cambridge, 1979).

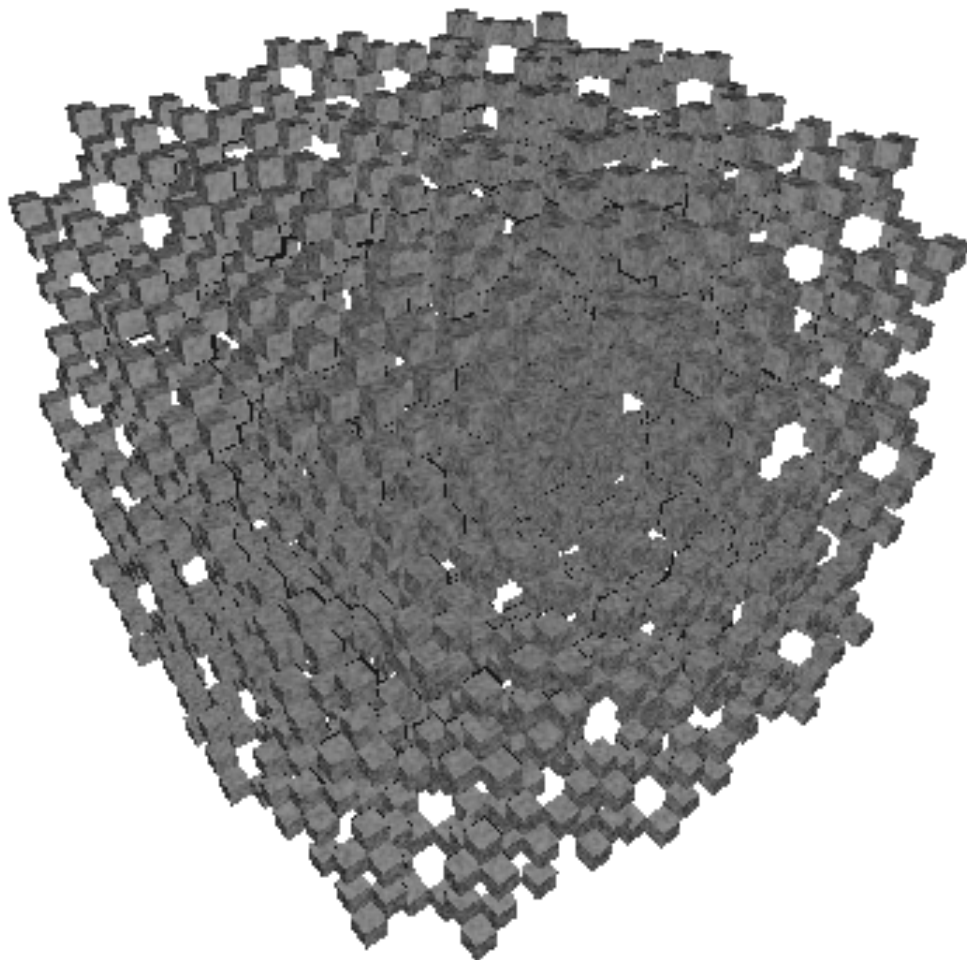


**Figure 23.** Three-dimensional HeartQuake image for  $M = \{0^31^32^3\}$ .

- [8] V. De Florio, “The HeartQuake Dynamic System,” *Complex Systems*, 9(2) (1995) 91–114.
- [9] S. Wolfram, *A New Kind of Science* (Wolfram Media Inc., Champaign, IL, 2002).
- [10] J. Smith, “Randscape: Complex Images from Simple Algorithms,” *Artificial Life*, 9(1) (2003).
- [11] D. E. Knuth, “Literate Programming,” *The Computer Journal*, 27 (1984) 97–111.